iScience

CellPress
OPEN ACCESS

Article

Cytoplasmic Dynein Functions in Planar Polarization of Basal Bodies within Ciliated Cells

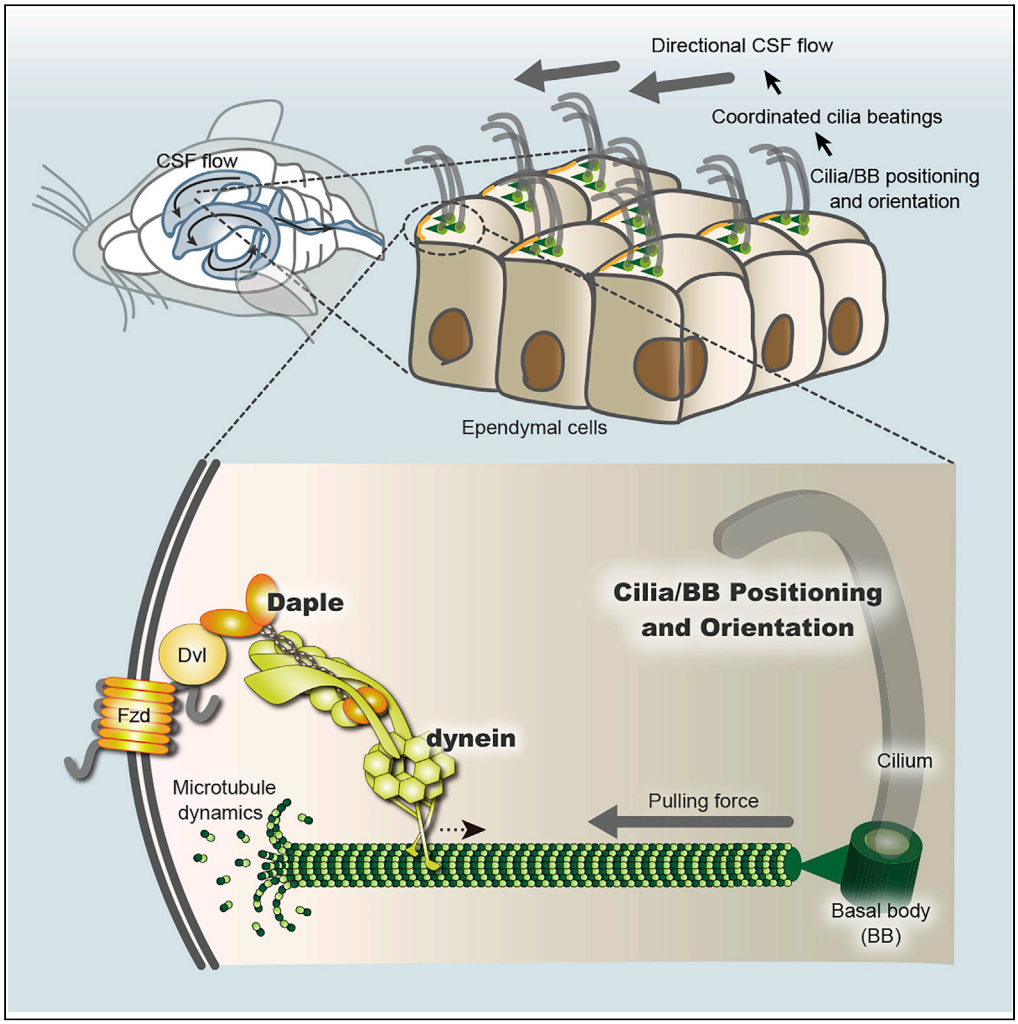

Maki Takagishi, Nobutoshi Esaki, Kunihiko Takahashi, Masahide Takahashi

m-stone@med.nagoya-u.ac.jp

HIGHLIGHTS

Daple anchors cytoplasmic dynein to the cell cortex of ependymal cells on LV wall

Cytoplasmic dynein is anchored to the Fzd6/Dvl1/Daple side of the cell cortex

Cytoplasmic dynein functions include BB positioning and orientation

Cortex-anchored dynein generates a pulling force on microtubules connected to BBs

Takagishi et al., iScience *23*, 101213
June 26, 2020
https://doi.org/10.1016/j.isci.2020.101213

iScience

CellPress
OPEN ACCESS

Article

Cytoplasmic Dynein Functions in Planar Polarization of Basal Bodies within Ciliated Cells

Maki Takagishi,[1,5,*] Nobutoshi Esaki,[1] Kunihiko Takahashi,[2,3] and Masahide Takahashi[1,4]

SUMMARY

Despite common consensus about the importance of planar cell polarity (PCP) proteins in tissue orientation, little is known about the mechanisms used by PCP proteins to promote planar polarization of cytoskeletons within individual cells. One PCP protein Fzd6 asymmetrically localizes to the apical cell membrane of multi-ciliated ependymal cells lining the lateral ventricular (LV) wall on the side that contacts cerebrospinal fluid flow. Individual ependymal cells have planar polarized microtubules that connect ciliary basal bodies (BBs) with the cell cortex of the Fzd side to coordinate cilia orientation. Here, we report that cytoplasmic dynein is anchored to the cell cortex of the Fzd side via an adapter protein Daple that regulates microtubule dynamics. Asymmetric localization of cortical dynein generates a pulling force on dynamic microtubules connected to BBs, which in turn orients BBs toward the Fzd side. This is required for coordinated cilia orientation on the LV wall.

INTRODUCTION

Cilia arise from basal bodies (BBs) docked on apical cell surfaces, and their orientation is determined by planar polarity at the apical cell cortex. Coordinated beatings of multiple motile cilia with coordinated orientation generate directional fluid flow on the tissue surface. This enables brain ventricle circulation of cerebrospinal fluid (CSF), protective airway mucus clearance, and ovarian tube egg transportation (Marshall and Kintner, 2008). Perturbation of coordinated cilia orientation results in hydrocephalus, chronic obstructive pulmonary disease (COPD), and female infertility (Meunier and Azimzadeh, 2016). Ependymal cells that line the lateral ventricular (LV) wall have multiple motile cilia that are oriented toward and beat parallel to the flow of CSF (Mirzadeh et al., 2010; Figures 1A and 1C). In response to the initial passive CSF flow, planar cell polarity (PCP) protein, Vangl2, is required for the rotational orientation of BB/cilia within individual ependymal cells (Guirao et al., 2010). Mutations in other PCP genes (*Celsr, Dvl, and Daple*) also disrupt BB/cilia orientation and ependymal flow, which results in stagnant CSF and hydrocephalus (Tissir et al., 2010; Boutin et al., 2014; Ohata et al., 2014; Takagishi et al., 2017). As such, PCP proteins are essential for the orientation of ependymal cilia and consequently for the directional active flow of CSF (Guirao et al., 2010; Ohata and Alvarez-Buylla, 2016).

Tissue strain stimulates subcellular asymmetric accumulation of core PCP proteins (Fzd/Dvl and Vangl/Pk) in animals (Carvajal-Gonzalez et al., 2016). PCP proteins are known to organize microtubule polarization, which establishes the planar polarity of cells (Matis et al., 2014; Chien et al., 2015). In tracheal multi-ciliated cells, microtubules show plane polarization at the apical cell cortex and this contributes to BB orientation (Vladar et al., 2012; Kunimoto et al., 2012; Chien et al., 2015). Growing ends of microtubules are localized asymmetrically at the side of the cell cortex, where Fzd accumulates (Vladar et al., 2012; Butler and Wallingford, 2017). However, the mechanisms employed by PCP proteins that are responsible for microtubule organization and cilia orientation remain unclear.

During Wnt signaling, a Wnt ligand binds to the seven-pass transmembrane receptor Fzd, which then recruits a scaffold protein Dvl that induces downstream signaling (Schulte and Bryja, 2007). We have previously reported a loss of microtubule polarization in mice that are deficient for a Dvl-binding protein Daple (Takagishi et al., 2017). In light of these findings, we proceeded to study how Fzd engages growing ends of microtubules and regulates BB orientation.

[1]Department of Pathology, Nagoya University Graduate School of Medicine, Nagoya, Aichi 466-8550, Japan

[2]Department of Biostatistics, Nagoya University Graduate School of Medicine, Nagoya, Aichi 466-8550, Japan

[3]Department of Biostatistics, M&D Data Science Center, Tokyo Medical and Dental University, Bunkyo-ku, Tokyo 113-8510, Japan

[4]International Center for Cell and Gene Therapy, Fujita Health University, Toyoake, Aichi 470-1192, Japan

[5]Lead Contact

*Correspondence: m-stone@med.nagoya-u.ac.jp

https://doi.org/10.1016/j.isci.2020.101213

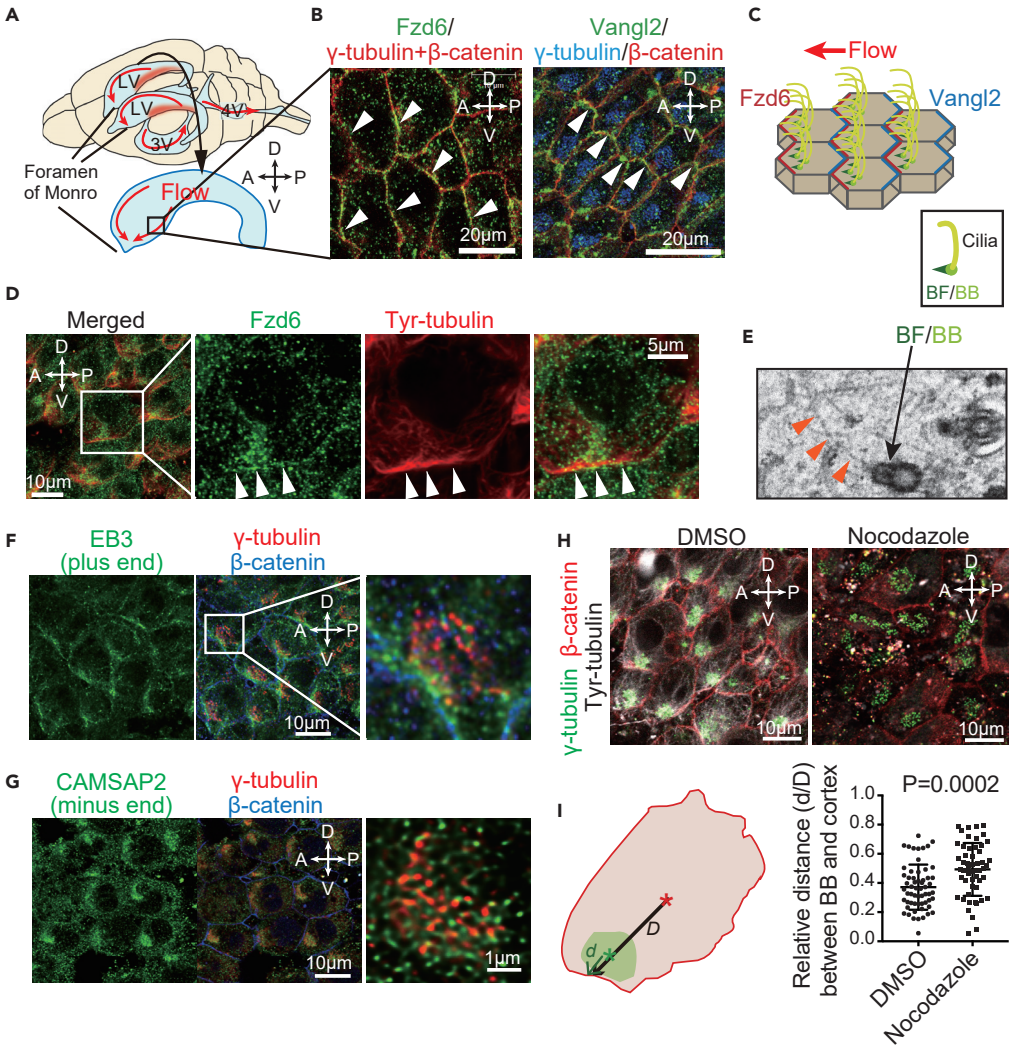

Figure 1. Dynamic Microtubule Changes Took Place at the Fzd Side of the Cell Cortex to Modulate BB Positioning at Ependymal Cells

(A) Illustration of directional CSF flow in the brain ventricles. CSF (red arrow) is produced at the choroid plexus (red area) in the posterior region of the lateral ventricle (LV) and outflows through the Foremen of Monro at the anterior-ventral region of the LV, toward the third ventricle (3V) and fourth ventricle (4V). The illustration below represents the surface of a dissected right distal LV wall. Microscopy images of the boxed area are shown for all experiments. A, anterior; P, posterior; D, dorsal; V, ventral sides of the brain.

(B) Confocal images of the LV wall at the horizontal plane show the apical cell cortex of ependymal cells. Whole mounts of LV wall tissue were stained with antibodies against Fzd6 (left panel, green), Vangl2 (right panel, green), γ-tubulin (basal bodies, red in the left panel or blue in the right panel), and β-catenin (cell boundary, red). Arrowheads indicate asymmetric localization of Fzd6 at the anterior-ventral side (left panel) or Vangl2 at the posterior-dorsal side (right panel) of the apical cell membrane of ependymal cells.

(C) Representation of ependymal cells lining the LV wall, the orientation of multiple cilia (yellow), and asymmetric localization of Fzd6 (red) and Vangl2 (blue) at the apical cell membrane, parallel to surface CSF flow (red arrow). BF (basal foot, green) and BB (basal body, light green) located at the base of cilia are rotationally oriented toward the Fzd side.

(D) Whole-mount staining of the LV wall with antibodies against Fzd6 (green) and tyrosinated (Tyr)-tubulin (red). Arrowheads indicate sites of Fzd6 accumulation with tyrosinated tubulin located at the ventral side of the apical cell membrane.

(E) Image of an ependymal cell at the LV wall obtained by electron microscopy shows filaments (arrowheads) connected to the BF/BB structure.

(F) Whole-mount staining of the LV wall with antibodies against EB3 that marks the microtubule plus end (green), γ-tubulin (red), and β-catenin (blue).

Figure 1. *Continued*

(G) Whole-mount staining of the LV wall with antibodies against CAMSAP2 that marks the microtubule minus end (green), γ-tubulin (red), and β-catenin (blue) antibodies.

(H) Tissue explants from the LV wall were incubated with DMSO or Nocodazole (10 μM) for 24 h and stained with antibodies against tyrosinated tubulin (white), γ-tubulin (green), and β-catenin (red).

(I) Illustration (left) shows the measurement of the distance between the cell cortex and the center of the BB cluster (*d*) or the cell surface (*D*). The ratio of *d/D* was represented as the relative distance between the BB cluster and the cell cortex. Quantification (right) is represented as the mean ± SEM of 54 cells from three mice in each treatment group (representative microscopy data shown in [H]). Data are represented for *d/D* with DMSO and Nocodazole treatment.

We have demonstrated here that Daple anchors cytoplasmic dynein to the cell cortex of ependymal cells on the LV wall. Cytoplasmic dynein is a cytoskeletal motor protein that traverses microtubules toward the microtubules' minus end that lies within the microtubule-organizing center (Roberts et al., 2013). Cell cortex-anchored dynein generates a pulling force on astral microtubules that are connected to the spindle pole during anaphase (Laan et al., 2012). We have found that cytoplasmic dynein is anchored to the Fzd6/Dvl1/Daple side of the cell cortex and functions in BB positioning and orientation. Our data suggest that cortex-anchored dynein at the Fzd/Dvl/Daple side of the cell cortex generates a pulling force on microtubules connected to BBs and utilizes microtubule dynamics to control positioning and rotation of BBs.

RESULTS

Planar Polarization of Microtubules in Ependymal Cells

Within the LV, CSF flows from the posterior choroid plexus toward the anterior-ventral foramen of Monro (Figure 1A). Ependymal cells lining LV walls display asymmetric accumulation of PCP proteins, with multiple cilia oriented along the direction of CSF flow (Guirao et al., 2010; Ohata and Alvarez-Buylla, 2016). A core PCP protein, Fzd6, was asymmetrically localized to the anterior-ventral side of the apical cell membrane, downstream of CSF flow (Figures 1B and 1C). A different core PCP protein, Vangl2 was specifically localized on the opposite side (Figures 1B and 1C).

Immunofluorescence of cells stained with antibodies against tyrosinated α-tubulin showed that newly polymerized dynamic microtubules were located at the Fzd6 side of the cell cortex (Figure 1D). Microtubule-like filaments were observed by electron microscopy to be connected to a protrusion from the BB that indicates cilia direction in ependymal cells, known as the basal foot (BF) (Figure 1E). Tyrosinated tubulin recruits microtubule plus-end-tracking proteins (+TIPs) at the microtubule plus end (Peris et al., 2006). EB3 is a +TIP that co-localized with tyrosinated tubulin at the anterior-ventral side of the ependymal cell cortex (Figure 1F). In contrast, CAMSAP2, a microtubule minus-end binding protein, was attached to the ciliary base (Figure 1G). To determine the functional role of a microtubule connection from BB to the Fzd side of the cell cortex, tissue explants from the LV wall were treated with nocodazole, an inhibitor of microtubule polymerization. Microtubule dynamics were suppressed by nocodazole treatment and resulted in reduced tyrosinated tubulin with the BB positioned toward the anterior-ventral side of the cell cortex (Figure 1H). Measured distance between the BB and the cell cortex was significantly larger ($p = 0.0002$) under nocodazole treatment (0.4929 ± 0.02465, $n = 54$) compared with the control (0.3713 ± 0.02013, $n = 59$) (Figure 1I). These results suggest that BB positioning takes place through the extension of planar polarized microtubules from BB at its minus end toward the Fzd-side cell cortex at the plus end.

Daple Modulates Microtubule Dynamics at the Fzd Side of the Cell Cortex

Dvl is an Fzd-binding protein that acts as one of the core PCP proteins and is involved with cilia orientation in ependymal cells (Ohata et al., 2014: Yang and Mlodzik, 2015). The three isoforms of Dvl (Dvl1-3) are localized differently in multi-ciliated cells (Vladar et al., 2012). Dvl2 was found to be localized at the BB in ependymal cells (Ohata et al., 2014), whereas Dvl1 co-localized with Daple at the anterior-ventral side of the apical cell cortex (Figure 2A). Daple is a Dvl-associating scaffold protein that functions in non-canonical Wnt signaling and is required for BB positioning and orientation (Ishida-Takagishi et al., 2012; Takagishi et al., 2017). We have previously found that Daple co-localizes with Fzd6 at the anterior-ventral side of ependymal cells and is required for planar polarization of microtubules (Takagishi et al., 2017). In this study, we observed co-localization of Fzd6, Dvl1, and Daple with tyrosinated tubulin at the anterior-ventral side of ependymal cells (Figure 2B). Additionally, at the LV wall of both wild-type ($Daple^{+/+}$) and Daple knockouts ($Daple^{-/-}$), tyrosinated tubulin was also localized to the cell cortex in ependymal cells with asymmetric accumulation of Fzd6 (Figure 2C). $Daple^{-/-}$ ependymal cells significantly decreased ($p < 0.0001$) localization of tyrosinated tubulin at the Fzd6 side of the cell cortex (0.9785 ± 0.04882, $n =$

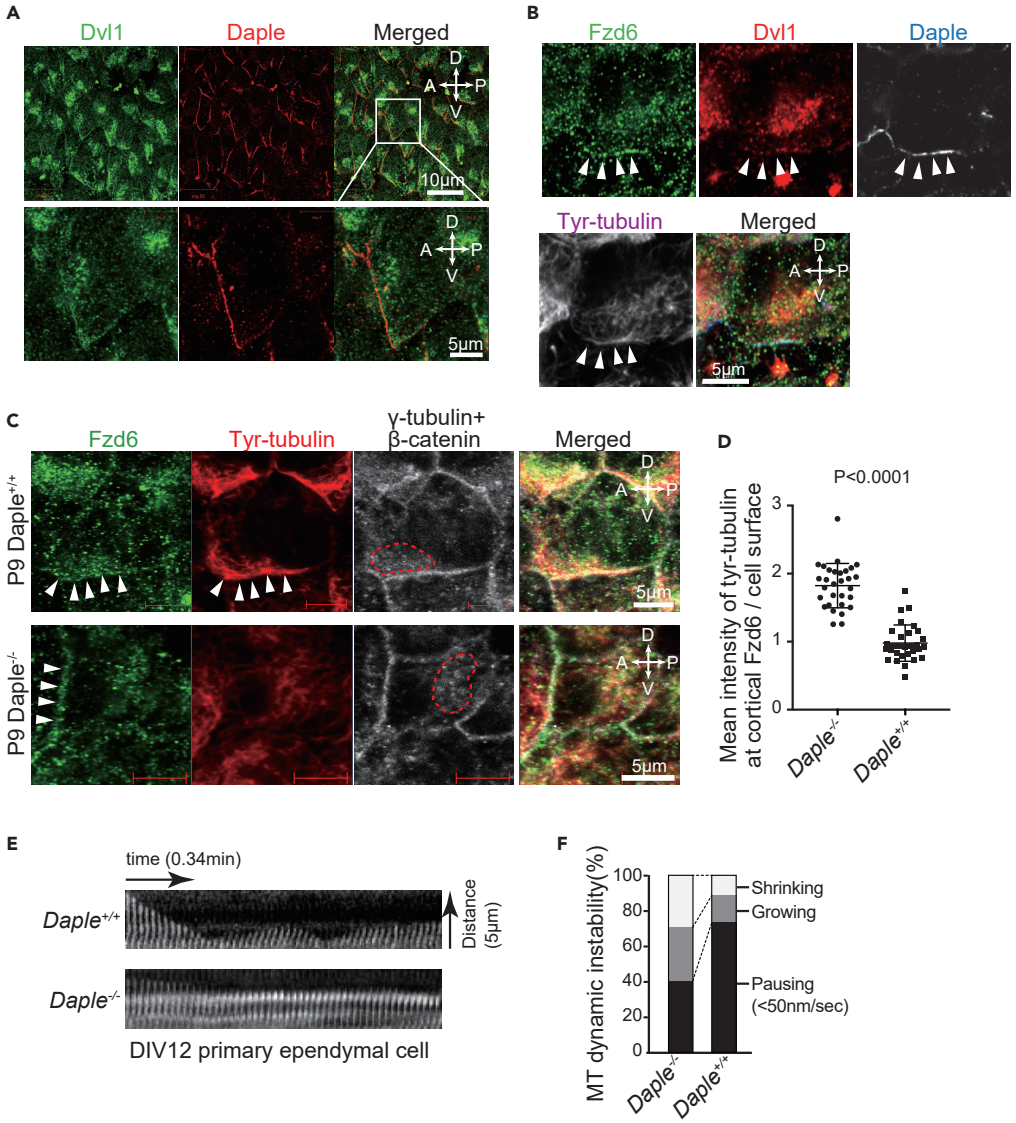

Figure 2. Daple Localizes to the Fzd/Dvl Side of the Cell Cortex and Regulates Microtubule Dynamics

(A) Whole-mount staining of the LV wall with antibodies against Dvl1 (green) and Daple (red). The enlarged image of the indicated box area is shown below.

(B) Whole-mount staining of the LV wall with antibodies against Fzd6 (green), Dvl1 (red), Daple (white/blue), and tyrosinated tubulin (white/magenta). Each panel shows the apical surface of the ependymal cells. Arrowheads indicate sites of co-localization of Fzd6, Dvl1, and Daple with tyrosinated tubulin at the cell cortex.

(C) Confocal microscopy images of the apical surface of *Daple*$^{+/+}$ or *Daple*$^{-/-}$ ependymal cells on the LV wall stained with antibodies against Fzd6 (green), tyrosinated tubulin (red), and γ-tubulin or β-catenin (white). Arrowheads indicate the accumulation of Fzd6 or tyrosinated tubulin at the cell cortex. Dashed lines indicate BB clusters.

(D) Accumulation of tyrosinated tubulin at the Fzd6 side of the cell cortex was quantified for *Daple*$^{+/+}$ and *Daple*$^{-/-}$ ependymal cells. The mean intensity of tyrosinated tubulin at the Fzd6 area of the cell cortex was normalized against the mean intensity of tyrosinated tubulin for the entire cell surface area. Normalized intensities are plotted as mean values ± SEM for 30 ependymal cells, sampled from three mice in each group.

(E) Kymographs of single microtubules from *Daple*$^{+/+}$ or *Daple*$^{-/-}$ ependymal cells. The tips of EMTB-EGFP at the cell edge were monitored by fluorescence time-lapse microscopy imaging, see also Videos S1 and S2.

(F) Quantification of the state of microtubule dynamics in *Daple*$^{+/+}$ or *Daple*$^{-/-}$ ependymal cells. Shrinking, growing, and pausing (pause defined as > 0.1 μm/2 s) states of 30 microtubules were measured over 2.55 min for each group. Values are represented in Table S1.

30) relative to *Daple*$^{+/+}$ (1.824 ± 0.05945, n = 30) (Figure 2D). This suggests that Daple is involved in the recruitment of the end of the microtubule where dynamic changes take place to the Fzd side of the cell cortex.

As *Daple*$^{-/-}$ ependymal cells had decreased tyrosinated tubulin (Takagishi et al., 2017), we proceeded to determine the effect of Daple deficiency on microtubule dynamics in ependymal cells. Polymerization dynamics at the end of individually labeled microtubules were monitored at the cell cortex in primary cultured ependymal cells expressing E-MAP-115 microtubules-binding domain (EMTB)-EGFP (Faire et al., 1999). In *Daple*$^{+/+}$ ependymal cells, microtubules at the cell cortex showed continuous growth and shrinkage (Video S1). In contrast, microtubules in *Daple*$^{-/-}$ ependymal cells showed only minimal growth and shrinkage (Video S2). The changes at the end of a representative microtubule are plotted against time (Figure 2E). The wild-type *Daple*$^{+/+}$ microtubule frequently oscillated between growth and shrinkage, whereas *Daple*$^{-/-}$ microtubules exhibited minimal oscillation. Quantification of the changes in microtubule dynamics showed that *Daple*$^{-/-}$ had significant increases ($p < 0.0001$) in time spent in the pausing state and decreased ($p < 0.0001$) time spent in the shrinking or growing state (Figure 2F and Table S1). These results suggest that Daple promotes dynamic microtubule changes, which explains the co-localization of Daple with tyrosinated tubulin at the Fzd side of the cell cortex. This further begs the question of how local microtubule dynamics regulate BB positioning.

Cytoplasmic Dynein Is Anchored to the Cortex in Ependymal Cells

In mitotic cells, cytoplasmic dynein anchored at the cell cortex captures the dynamic end of the microtubule and generates a pulling force on astral microtubules connected to the spindle pole (Laan et al., 2012; McNally, 2013). During ependymal cell maturation (P7–P15), BBs are strongly pulled toward the anterior side of the cell cortex, where Fzd has accumulated (Hirota et al., 2010, 2016). We hypothesized that dynein's pulling force was also generated on planar polarized microtubules that were connected to BBs. Whole-mount immunofluorescence imaging of the LV wall showed that dynein intermediated chain (IC) accumulates at the apical cell cortex, with tyrosinated tubulin on the anterior-ventral side of LV (Figure 3A). Dynein IC was also observed at the BB cluster.

Daple has also been reported as an adaptor protein of cytoplasmic dynein (Redwine et al., 2017). We used co-immunoprecipitation of LV tissue lysate to determine if Daple interacts with dynein. Dynein IC, heavy chain (HC), and Dvl1 co-immunoprecipitated with Daple (Figure 3B). Daple co-immunoprecipitated with dynein IC but Dvl1 did not (Figure 3C).

We visualized the localization of dynein and Daple mutants in primary cultured ependymal cells to obtain more information about dynein's anchoring proteins at the cell cortex. The N-terminal (NT) region of Daple binds to dynein (Redwine et al., 2017). Daple interacts with a heterotrimeric G-protein Gαi by binding to its Gαi-binding and activating (GBA) motif, and Dvl by binding to its C-terminal PSD95/Dlg/ZO-1 (PDZ)-binding motif (PBM) (Figure S1A; Aznar et al., 2015). Daple wild-type, ΔNT, and ΔGBA, but not ΔPBM, were localized at the cell cortex (Figure S1B). GFP-dynein was localized at the cell cortex with Daple wild-type (76.5%) or ΔGBA (67.5%) but not with Daple ΔNT (7.1%) or ΔPBM (6.5%) (Figures S1B and S1C and Table S2). These results suggest that PDZ binding of Daple is necessary for the anchoring of dynein to the cell cortex in ependymal cells. We observed the co-localization of dynein with Daple in the cortex of ependymal cells at the anterior-ventral side of the *Daple*$^{+/+}$ LV wall (Figure 3D). Dynein co-localization was abolished in the *Daple*$^{-/-}$ LV wall, with disrupted BB positioning and orientation (Takagishi et al., 2017). Taken together, these data indicated that Daple is required for anchoring of cytoplasmic dynein to the anterior-ventral side of the cell cortex.

Cytoplasmic Dynein Regulates BB Position and Orientation

To determine if cytoplasmic dynein is involved with BB positioning and orientation, tissue explants from the LV wall were treated with an inhibitor of cytoplasmic dynein, Dynarrestin (Höing et al., 2018). Dynarrestin treatment disrupted BB positioning and recruitment of tyrosinated tubulin to the cell cortex (Figure 4A) and significantly increased ($p < 0.0001$) the distance between the BB cluster and the cell cortex (0.5381 ± 0.01875, n = 58) relative to the DMSO control (0.3713 ± 0.02013, n = 59) (Figure 4B). Rotational BB orientation was visualized by immunofluorescence staining with antibodies against FGFR1 oncogene partner (FOP) and γ-tubulin (Figure 4C) and was defined as the angle from FOP to γ-tubulin dots (Figure 4D) (Labedan et al., 2016). Distribution of BB angles was calculated as circular variance (*V*) and was found to be

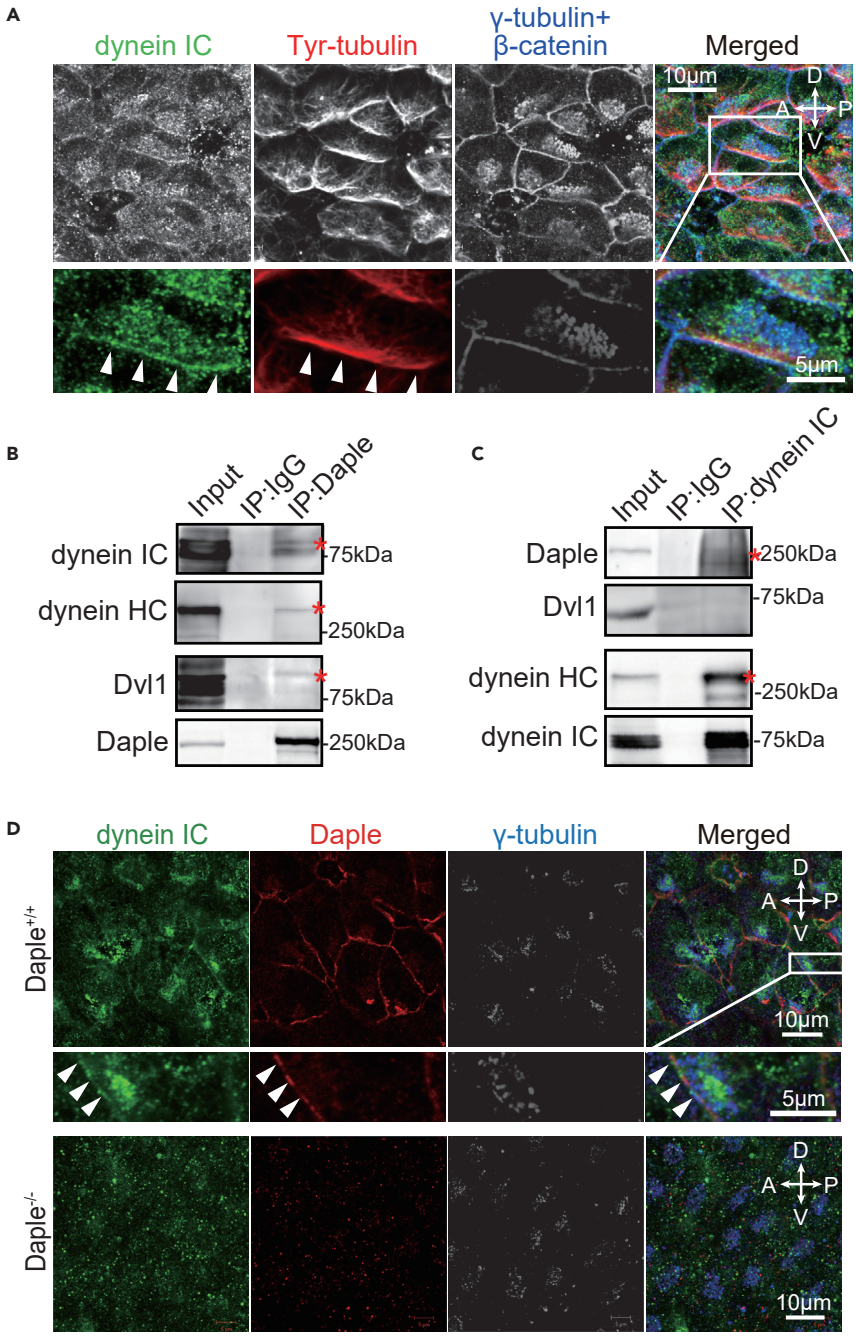

Figure 3. Cytoplasmic Dynein Was Anchored to the Cell Cortex by Daple in Ependymal Cells

(A) Whole-mount stain of the LV wall with antibodies against dynein intermediate chain (IC, green), tyrosinated tubulin (red), and γ-tubulin or β-catenin (blue). Panels below represent a high magnification of the box shown in the right panel. Arrowheads indicate sites of accumulation of dynein IC with tyrosinated tubulin at the cell cortex.

(B) Lysates of tissue from the LV wall were immunoprecipitated with IgG or anti-Daple antibody. The total cell lysate (Input) and the immunoprecipitates were blotted with anti-dynein IC, anti-dynein HC, anti-Dvl1, or anti-Daple antibodies, as indicated on the left of each panel. Asterisks indicate the bands of co-immunoprecipitated proteins.

(C) Tissue lysates from the LV wall were immunoprecipitated with IgG or anti-dynein IC antibody and immunoblotted with respective antibodies as indicated on the left. Asterisks indicate the bands of proteins that co-immunoprecipitated together.

(D) Whole-mount *Daple*$^{+/+}$ and *Daple*$^{-/-}$ tissue stained with antibodies against dynein IC (green), Daple (red), and γ-tubulin (blue) at the LV wall. Arrowheads indicate sites of co-localization of dynein IC with Daple at the cell cortex.

See also Figure S1 and Table S2.

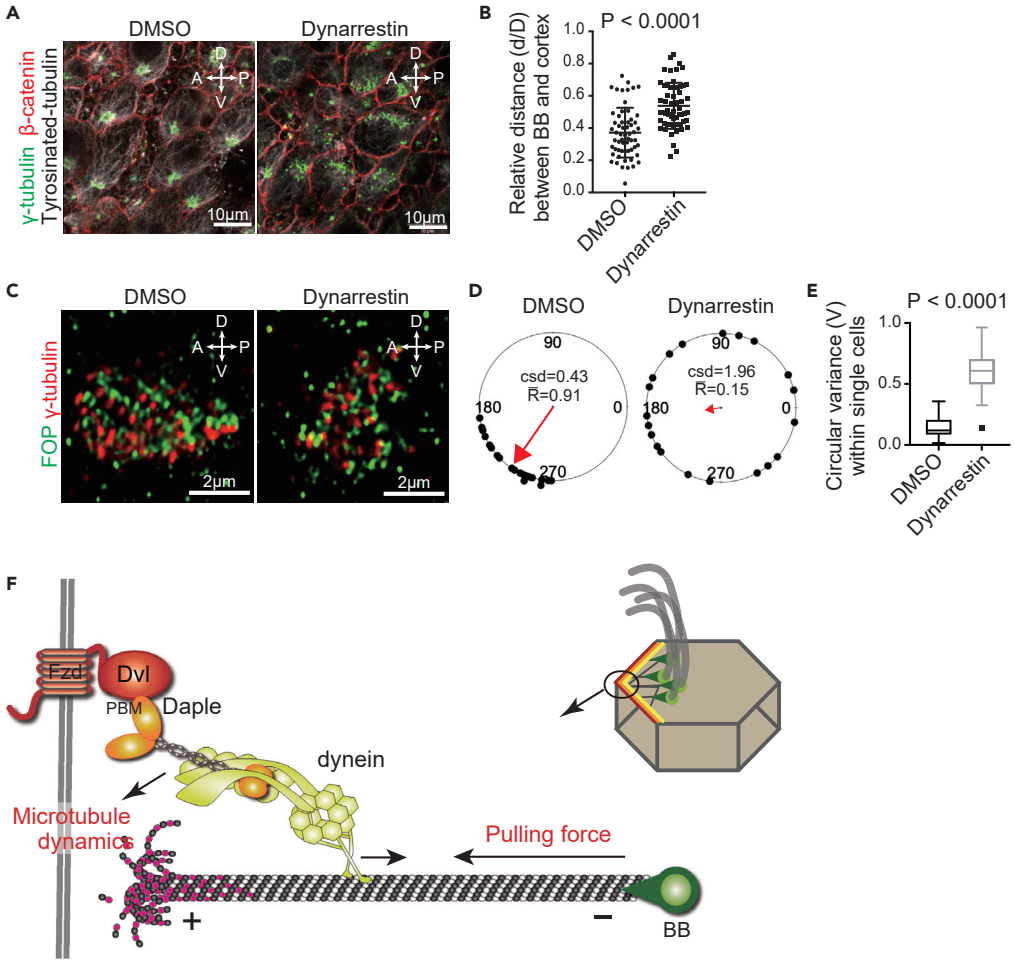

Figure 4. Positioning and Orientation of the BB Were Reduced by Inhibition of Cytoplasmic Dynein

(A) Tissue explants from the LV wall were treated for 24 h with DMSO or Dynarrestin (20 μM), an inhibitor of cytoplasmic dynein. Tissue explants were stained with antibodies against γ-tubulin (green), β-catenin (red), and tyrosinated tubulin (white).

(B) Quantification of the ratios of relative distance (d/D) between the BB cluster and the cell cortex. Data are represented as the mean ± SEM of 58 cells from three mice in each group from microscopy data represented in (A).

(C) Tissue explants from the LV wall were treated for 12 h with DMSO or Dynarrestin (20 μM). Representative images of the LV explants stained with anti-FOP (green) and anti-γ-tubulin (red) antibodies are shown.

(D) The angles from FOP to γ-tubulin dots (n = 20) shown in (C) were plotted on circular diagram in each cell. The red vector is the mean resultant vector of the individual angle data. $\overline{R}$, the length of mean resultant vector; csd, circular standard deviation.

(E) Circular variance ($V = 1 - \overline{R}$) within single ependymal cells was calculated to represent a distribution of BB angles (n = 17–22 BBs in each of the 43 ependymal cells from three mice per treatment group). The data in box plots are given as medians, 25th–75th percentiles, ranges, and outliers.

(F) A proposed model for molecular positioning of BB. Dvl binds to Fzd on the cell membrane and captures an adaptor protein Daple through its PBM to anchor cytoplasmic dynein to the cell cortex. Daple/dynein at the cell cortex can promote dynamic microtubule cycling and generates a pulling force on microtubules connected to BBs.

significantly larger ($p < 0.0001$) under Dynarrestin treatment (0.5935 ± 0.02395, n = 43) relative to the DMSO control (0.1412 ± 0.0126, n = 43) (Figure 4E). These data suggest that cytoplasmic dynein also regulates BB positioning and orientation in ependymal cells.

DISCUSSION

The role that PCP proteins play in microtubule polarization has long been a subject of speculation. It was widely assumed that downstream cytoplasmic molecules of Wnt/Fzd signaling regulate microtubule

remodeling; however, molecular mechanisms that regulate microtubule polarity remain to be elucidated. Here, we used ependymal ciliated cells in well-polarized LV wall tissue as a model and found that core PCP proteins Fzd/Dvl and Daple anchor dynein to the cell cortex and generate a pulling force on dynamic microtubules to exert force on BBs (Figure 4F). As such, BB positioning and cilia orientation are regulated at the molecular level by PCP proteins.

Translational BB position is spatiotemporally altered in ependymal cells at the LV wall during development and aging (Hirota et al., 2016). We have shown that stable tyrosinated tubulin localizes to the Fzd side of the cell cortex in ependymal cells (Figure 1D). Stable tyrosinated tubulin reflects microtubules at a state of dynamic equilibrium and includes tubulin dimer polymerization and depolymerization. Dynein at the cortex generates a pulling force on depolymerizing microtubules toward the cell cortex (Laan et al., 2012). On the contrary, microtubules undergoing growth can generate a pushing force (Vleugel et al., 2016). Both shrinking and growing of microtubules were suppressed in Daple-deficient ependymal cells (Figure 2F), which led to the disruption of translational BB position (Takagishi et al., 2017). These findings provide evidence for a model where continuous microtubule dynamics fine-tune the BB position by modulating the distance between the BB and the cell cortex.

BB position plays an important role in the rotational orientation of cilia. Translational positioning and rotational orientation of BB are established at around the same developmental stage, during P9 (Hirota et al., 2010). We have shown that treatment with a dynein inhibitor suppressed not only BB positioning but also its orientation (Figure 4). During translational positioning, dynein anchored on the Fzd side can generate a pulling force on the depolymerizing microtubules connected to the BF. The pulling force enables the orientation of the BF toward the Fzd side and leads to the rotational orientation of BBs.

Having found that Daple modulated microtubule dynamics at the Fzd side of the cell cortex (Figures 2C–2F), we proceeded to define the molecular mechanisms involved in this process. Dynein that is anchored to the cell cortex is able to capture the plus end of microtubules and control microtubule dynamics (Laan et al., 2012). As we observed that dynein inhibition decreased tyrosinated tubulin in ependymal cells (Figure 4A), we hypothesized that Daple might act through anchored dynein to promote dynamic cycling of microtubules at the cell cortex in ependymal cells.

It is known that core PCP proteins are also involved in the orientation of hair bundles on auditory sensory cells (Ezan and Montcouquiol, 2013). It has previously been reported that Daple regulates cilia orientation not only in multi-ciliated cells at the LV wall or in the trachea but also in hair cells of the auditory system (Takagishi et al., 2017; Siletti et al., 2017). In auditory sensory cells, Daple is asymmetrically localized at the cell cortex, on the same side as Fzd/Dvl. Interestingly, despite normal localization of Dvl and Gαi, Daple knockout mice showed disrupted kinocilium positioning in hair cells (Siletti et al., 2017). As microtubules and dynein regulate BB positioning of the kinocilium (Lu and Sipe, 2016), it is possible that Daple may anchor dynein to pull the BB of the kinocilium toward the Fzd/Dvl side of the cell cortex. This hypothesis is supported by evidence from a yeast two-hybrid assay, which showed a cofactor of dynein, dynactin, interacts with Daple in auditory sensory cells (Siletti et al., 2017). Taken together, these studies suggest that Daple may play an important role in various tissues in the PCP protein-mediated regulation of BB positioning through cortical dynein.

Critically, the data here demonstrate that the C-terminal PDZ-binding motif of Daple is essential for the anchoring of Daple and dynein to the cortex (Figure S1). A nonsense mutation E1949GfsX26 in *DAPLE* is found in patients with hydrocephalus and causes termination at 1973, which results in the loss of the PDZ-binding motif (Drielsma et al., 2012). Daple-deficient mice showed loss of dynein at the cell cortex (Figure 3E), and lack of coordinated cilia orientation and movement on the LV wall, resulting in stagnant CSF flow and hydrocephalus (Takagishi et al., 2017). This mouse model study not only improves our understanding of mechanisms underlying cilia orientation but may also provide insight into the etiology of human hydrocephalus.

Limitation of the Study

In this study, we cultured ependymal cells to observe microtubule dynamics and the cortical localization of dynein with Daple mutants (Figures 2E, 2F, and S1). However, these cultured ependymal cells could not be perfectly polarized under no-flow conditions (Guirao et al., 2010). To overcome this limitation, future

experiments should assess microtubule dynamics and the effects of Daple mutants in well-polarized ependymal cells with directional flow *in vitro* or *in vivo*.

Resource Availability

Lead Contact

Further information and requests for resources and reagents should be directed to and will be fulfilled by the Lead Contact, Maki Takagishi (m-stone@med.nagoya-u.ac.jp).

Materials Availability

Daple ΔGBA, and ΔPBM-expression plasmids were newly generated in this study. These plasmids are available from the Lead Contact without restriction.

Data and Code Availability

This study did not generate datasets/code.

METHODS

All methods can be found in the accompanying Transparent Methods supplemental file.

SUPPLEMENTAL INFORMATION

Supplemental Information can be found online at https://doi.org/10.1016/j.isci.2020.101213.

ACKNOWLEDGMENTS

The ES cell line used for Daple knockout mice was generated by the KOMP (www.komp.org). We thank Shindo, A. (Nagoya University) for technical advice on cell imaging and Goshima, G. (Nagoya University) for technical advice and helpful discussions on microtubule dynamics. We would also like to thank Wallingford, J.B. (University of Texas at Austin) for helpful discussions. This work was supported by Grant-in-Aid for Scientific Research (S) 26221304 to M. Takahashi, Grant-in-Aid for Young Scientists (B) 17K15593 and Naito Foundation to M. Takagishi.

AUTHOR CONTRIBUTIONS

Conceptualization, Methodology, Investigation, Writing, Project administration, Funding acquisition, and Supervision, M. Takagishi; Investigation and Resources, N.E.; Formal Analysis, K.T.; Funding acquisition, Resources, and Supervision, M. Takahashi.

DECLARATION OF INTERESTS

The authors declare no competing interests.

Received: February 10, 2020
Revised: April 26, 2020
Accepted: May 27, 2020
Published: June 26, 2020

REFERENCES

Aznar, N., Midde, K.K., Dunkel, Y., Lopez-Sanchez, I., Pavlova, Y., Marivin, A., Barbazán, J., Murray, F., Nitsche, U., Janssen, K.P., et al. (2015). Daple is a novel non-receptor GEF required for trimeric G protein activation in Wnt signaling. Elife *4*, e07091.

Boutin, C., Labedan, P., Dimidschstein, J., Richard, F., Cremer, H., André, P., Yang, Y., Montcouquiol, M., Goffinet, A.M., and Tissir, F. (2014). A dual role for planar cell polarity genes in ciliated cells. Proc. Natl. Acad. Sci. U S A *111*, E3129–E3138.

Butler, M.T., and Wallingford, J.B. (2017). Planar cell polarity in development and disease. Nat. Rev. Mol. Cell Biol. *18*, 375–388.

Carvajal-Gonzalez, J.M., Mulero-Navarro, S., and Mlodzik, M. (2016). Centriole positioning in epithelial cells and its intimate relationship with planar cell polarity. Bioessays *38*, 1234–1245.

Chien, Y.H., Keller, R., Kintner, C., and Shook, D.R. (2015). Mechanical strain determines the axis of planar polarity in ciliated epithelia. Curr. Biol. *25*, 2774–2784.

Drielsma, A., Jalas, C., Simonis, N., Désir, J., Simanovsky, N., Pirson, I., Elpeleg, O., Abramowicz, M., and Edvardson, S. (2012). Two novel CCDC88C mutations confirm the role of DAPLE in autosomal recessive congenital hydrocephalus. J. Med. Genet. *49*, 708–712.

Ezan, J., and Montcouquiol, M. (2013). Revisiting planar cell polarity in the inner ear. Semin. Cell Dev. Biol. *24*, 499–506.

Faire, K., Waterman-Storer, C.M., Gruber, D., Masson, D., Salmon, E.D., and Bulinski, J.C. (1999). E-MAP-115 (ensconsin) associates

dynamically with microtubules in vivo and is not a physiological modulator of microtubule dynamics. J. Cell Sci. *112*, 4243–4255.

Guirao, B., Meunier, A., Mortaud, S., Aguilar, A., Corsi, J.M., Strehl, L., Hirota, Y., Desoeuvre, A., Boutin, C., Han, Y.G., et al. (2010). Coupling between hydrodynamic forces and planar cell polarity orients mammalian motile cilia. Nat. Cell Biol. *12*, 341–350.

Hirota, Y., Meunier, A., Huang, S., Shimozawa, T., Yamada, O., Kida, Y.S., Inoue, M., Ito, T., Kato, H., Sakaguchi, M., et al. (2010). Planar polarity of multiciliated ependymal cells involves the anterior migration of basal bodies regulated by non-muscle myosin II. Development *137*, 3037–3046.

Hirota, Y., Sawada, M., Huang, S.H., Ogino, T., Ohata, S., Kubo, A., and Sawamoto, K. (2016). Roles of Wnt signaling in the neurogenic niche of the adult mouse ventricular-subventricular zone. Neurochem. Res. *41*, 222–230.

Höing, S., Yeh, T.Y., Baumann, M., Martinez, N.E., Habenberger, P., Kremer, L., Drexler, H.C.A., Küchler, P., Reinhardt, P., Choidas, A., et al. (2018). Dynarrestin, a novel inhibitor of cytoplasmic dynein. Cell Chem. Biol. *25*, 357–369.

Ishida-Takagishi, M., Enomoto, A., Asai, N., Ushida, K., Watanabe, T., Hashimoto, T., Kato, T., Weng, L., Matsumoto, S., Asai, M., et al. (2012). The Dishevelled-associating protein Daple controls the non-canonical Wnt/Rac pathway and cell motility. Nat. Commun. *3*, 859.

Kunimoto, K., Yamazaki, Y., Nishida, T., Shinohara, K., Ishikawa, H., Hasegawa, T., Okanoue, T., Hamada, H., Noda, T., Tamura, et al.. (2012). Coordinated ciliary beating requires Odf2-mediated polarization of basal bodies via basal feet. Cell *148*, 189–200.

Laan, L., Pavin, N., Husson, J., Romet-Lemonne, G., van Duijn, M., López, M.P., Vale, R.D., Jülicher, F., Reck-Peterson, S.L., and Dogterom, M. (2012). Cortical dynein controls microtubule dynamics to generate pulling forces that position microtubule asters. Cell *148*, 502–514.

Labedan, P., Matthews, C., Kodjabachian, L., Cremer, H., Tissir, F., and Boutin, C. (2016). Dissection and staining of mouse brain ventricular wall for the analysis of ependymal cell cilia organization. BioProtoc *6*, e1757.

Lu, X., and Sipe, C.W. (2016). Developmental regulation of planar cell polarity and hair-bundle morphogenesis in auditory hair cells: lessons from human and mouse genetics. Wiley Interdiscip. Rev. Dev. Biol. *5*, 85–101.

Marshall, W.F., and Kintner, C. (2008). Cilia orientation and the fluid mechanics of development. Curr. Opin. Cell Biol. *20*, 48–52.

Matis, M., Russler-Germain, D.A., Hu, Q., Tomlin, C.J., and Axelrod, J.D. (2014). Microtubules provide directional information for core PCP function. Elife *3*, e02893.

McNally, F.J. (2013). Mechanisms of spindle positioning. J. Cell Biol. *200*, 131–140.

Meunier, A., and Azimzadeh, J. (2016). Multiciliated cells in animals. Cold Spring Harb. Perspect. Biol. *8*, a028233.

Mirzadeh, Z., Han, Y.G., Soriano-Navarro, M., García-Verdugo, J.M., and Alvarez-Buylla, A. (2010). Cilia organize ependymal planar polarity. J. Neurosci. *30*, 2600–2610.

Ohata, S., Nakatani, J., Herranz-Pérez, V., Cheng, J., Belinson, H., Inubushi, T., Snider, W.D., García-Verdugo, J.M., Wynshaw-Boris, A., and Alvarez-Buylla, A. (2014). Loss of Dishevelleds disrupts planar polarity in ependymal motile cilia and results in hydrocephalus. Neuron *83*, 558–571.

Ohata, S., and Alvarez-Buylla, A. (2016). Planar organization of multiciliated ependymal (E1) cells in the brain ventricular epithelium. Trends Neurosci. *39*, 543–551.

Peris, L., Thery, M., Fauré, J., Saoudi, Y., Lafanechère, L., Chilton, J.K., Gordon-Weeks, P., Galjart, N., Bornens, M., Wordeman, L., et al. (2006). Tubulin tyrosination is a major factor affecting the recruitment of CAP-Gly proteins at microtubule plus ends. J. Cell Biol. *174*, 839–849.

Redwine, W.B., DeSantis, M.E., Hollyer, I., Htet, Z.M., Tran, P.T., Swanson, S.K., Florens, L., Washburn, M.P., and Reck-Peterson, S.L. (2017). The human cytoplasmic dynein interactome reveals novel activators of motility. Elife *6*, e28257.

Roberts, A.J., Kon, T., Knight, P.J., Sutoh, K., and Burgess, S.A. (2013). Functions and mechanics of dynein motor proteins. Nat. Rev. Mol. Cell Biol. *14*, 713–726.

Schulte, G., and Bryja, V. (2007). The Frizzled family of unconventional G-protein-coupled receptors. Trends Pharmacol. Sci. *28*, 518–525.

Siletti, K., Tarchini, B., and Hudspeth, A.J. (2017). Daple coordinates organ-wide and cell-intrinsic polarity to pattern inner-ear hair bundles. Proc. Natl. Acad. Sci. U S A *114*, E11170–E11179.

Takagishi, M., Sawada, M., Ohata, S., Asai, N., Enomoto, A., Takahashi, K., Weng, L., Ushida, K., Ara, H., Matsui, S., et al. (2017). Daple coordinates planar polarized microtubule dynamics in ependymal cells and contributes to hydrocephalus. Cell Rep. *20*, 960–972.

Tissir, F., Qu, Y., Montcouquiol, M., Zhou, L., Komatsu, K., Shi, D., Fujimori, T., Labeau, J., Tyteca, D., Courtoy, P., et al. (2010). Lack of cadherins Celsr2 and Celsr3 impairs ependymal ciliogenesis, leading to fatal hydrocephalus. Nat. Neurosci. *13*, 700–707.

Vladar, E.K., Bayly, R.D., Sangoram, A.M., Scott, M.P., and Axelrod, J.D. (2012). Microtubules enable the planar cell polarity of airway cilia. Curr. Biol. *22*, 2203–2212.

Vleugel, M., Kok, M., and Dogterom, M. (2016). Understanding force-generating microtubule systems through in vitro reconstitution. Cell Adh. Migr. *10*, 475–494.

Yang, Y., and Mlodzik, M. (2015). Wnt-Frizzled/planar cell polarity signaling: cellular orientation by facing the wind (Wnt). Annu. Rev. Cell Dev. Biol. *31*, 623–646.

iScience, Volume *23*

Supplemental Information

Cytoplasmic Dynein Functions in Planar Polarization of Basal Bodies within Ciliated Cells

Maki Takagishi, Nobutoshi Esaki, Kunihiko Takahashi, and Masahide Takahashi

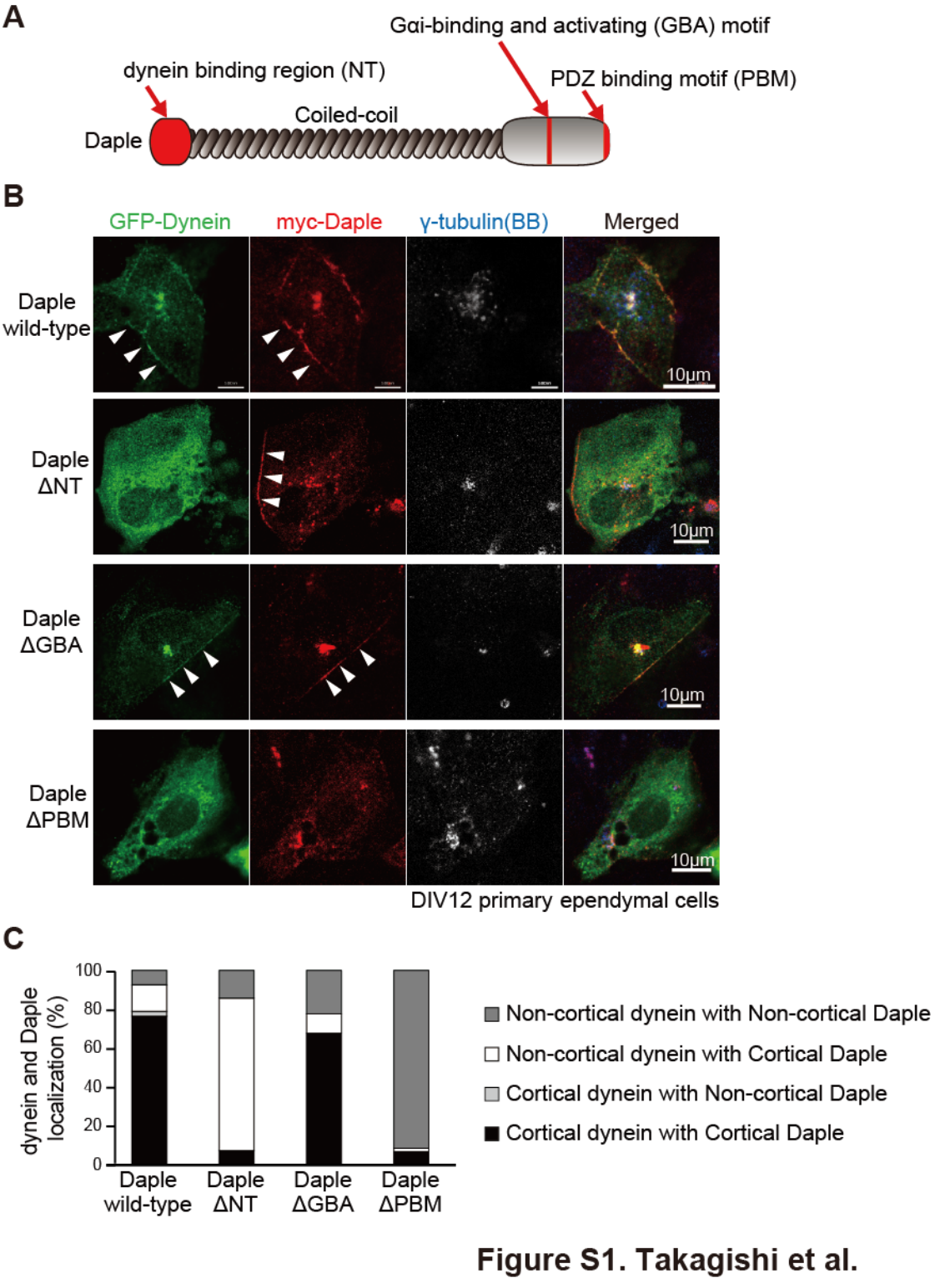

Figure S1. Localization of dynein with Daple mutants at the cell cortex in primary ependymal cells, related to Figure.3

(A) A schematic illustrating the protein domain organization of Daple. The N-terminal region (NT) of Daple interacts with dynein/dynactin. A long coiled-coil domain precedes the C-terminal region that includes a Gαi-binding and activating (GBA) motif and a PSD95/Dlg/ZO-1 (PDZ)-binding motif (PBM).

(B) Primary cultured ependymal cells were co-transfected with GFP-dynein heavy chain (green) and wild type myc-Daple or its mutants lacking the dynein binding (ΔNT), Gαi binding (ΔGBA), or PDZ-binding (ΔPBM) domains. These cells were stained with antibodies against myc (red) and γ-tubulin (white/blue). Arrowheads indicate the localization of dynein or Daple at the cell cortex.

(C) Localizations of GFP-dynein HC and myc-Daple mutants were classified into a cortical or non-cortical type and counted in the co-expression cells. The bar graph represents the percentage of dynein and Daple localization classified as cortical dynein with cortical Daple, cortical dynein with non-cortical Daple, non-cortical dynein with cortical Daple, or non-cortical dynein with non-cortical Daple for each Daple mutants. Values are represented in supplementary material, Table S2.

	Shrinking (%, Mean ± SEM)	**Growing (%, Mean ± SEM)**	**Pausing (%, Mean ± SEM)**
***Daple*$^{+/+}$**	30.05 ± 1.551	29.28 ± 1.638	40.68 ± 1.844
***Daple*$^{-/-}$**	15.47 ± 1.185	11.29 ± 1.182	73.24 ± 1.963
***P*-value**	<0.0001	<0.0001	<0.0001

Table S1. Microtubule dynamic instability parameters in Daple$^{+/+}$ or Daple$^{-/-}$ ependymal cells, related to Figure 2F.

	Daple wild-type	**Daple ΔNT**	**Daple ΔGBA**	**Daple ΔPBM**
Cortical dynein with Cortical Daple	76.47%	7.14%	67.50%	6.52%

Cortical dynein with Noncortical Daple	1.96%	0.00%	0.00%	0.00%
Noncortical dynein with Cortical Daple	13.73%	78.57%	10.00%	2.17%
Noncortical dynein with Noncortical Daple	7.84%	14.29%	22.50%	91.30%
Total counted cell number	51	28	40	46

Table S2. Dynein and Daple localization in GFP-dynein HC and myc-Daple mutants co-expressing ependymal cells, related to Figure S1 and Figure 3.

TRANSPARENT METHODS

Animal experiments

C57Bl/6J mice were used for whole-mount staining, ependymal cell culture, and LV explants cultures. ES cell clone (DEPD00564-1-E06) for Daple knockout mice purchased from the trans-NIH KOMP Repository (University of California Davis) (Skarnes et al, 2011). All mice were maintained with 12/12 h light/dark cycle and no more than 5 mice per cage. Both male and female mice were used for the experiments, and sex differences were not observed. All animal experiments were approved by the Animal Care and Use Committee of Nagoya University Graduate School of Medicine (approval no. 30364) and conducted in accordance with guidelines.

Plasmids

Mouse Daple cDNA encodes a 2009 amino acid protein, which was presented by Kikuchi, A. (Osaka University). The cDNAs of mDaple ΔNT (260-2009aa), ΔGBA (F1665A), and ΔPBM(1-2006aa) were subcloned into a pCAG vector with a myc tag. EGFP-dynein HC and EMTB-EGFP expression plasmids were generously provided by Kaibuchi, K. (Nagoya University) and Watanabe, T. (Fujita Health University).

Immunofluorescent staining

Whole-mount preparations of P9 LV wall tissue were fixed with methanol and 3.7% formaldehyde for 20 min, blocked with 10% donkey serum in PHEM buffer (PIPES, HEPES, EGTA, and $MgCl_2$) for 30 min and stained with antibodies overnight at 4°C. Primary antibodies were detected with secondary antibodies conjugated to Alexa Fluorophores. The apical surface

of ependymal cells was imaged using a confocal laser scanning microscope LSM700 (Zeiss) or A1 Rsi (Nikon) for super-resolution images.

Electron microscopy

P9 LV wall tissues were fixed using 2% glutaraldehyde with 2% paraformaldehyde and 1% osmium tetroxide. Ethanol-dehydrated tissues were displaced into propylene oxide and embedded in an epoxy resin. Tissue slices were sectioned (80 nm thickness) with an EM UC7i ultramicrotome (Leica) and counterstained with uranyl acetate and lead citrate. Images of the apical cell cortex of ependymal cells were obtained using a JEM-1400 (JEOL) electron microscope.

Ependymal cell culture

LV walls from P1 mouse brains were collected and the suspended cells with trypsin-EDTA were cultured in a laminin-coated flask for 3 days. Radial glial cells were plated on poly-L-lysine and laminin-coated coverslips and differentiated into ciliated ependymal cells by serum starvation. Ciliated ependymal cells were transfected with myc-Daple and EGFP-Dynein HC constructs at 11 days after differentiation using Lipofectamine 2000 (Invitrogen).

Microtubule dynamics assay

Cultured ependymal cells isolated from Daple$^{+/+}$ or Daple$^{-/-}$ mice were transfected with EMTB-EGFP 10 days after differentiation using Lipofectamine 2000 (Invitrogen). The EGFP-labeled growing tip of microtubules was monitored by confocal microscopy (LSM700) of the cell cortex 2 days post-transfection. Time-lapse series of confocal images were acquired at 2.04 sec intervals to tracking individual movements of 30 EMTB-EGFP-labeled microtubules in Daple$^{+/+}$ or Daple$^{-/-}$ ependymal cells. Kymographs of individual microtubules were obtained using digital linearization, and are represented from left to right.

Immunoprecipitation and western blotting

LV wall tissues were obtained from 20 mice at P9. LV wall tissues were lysed in PHEM buffer (50 mM PIPES, 50 mM HEPES, 1 mM EDTA, 2 mM $MgSO_4$, 1% Triton X-100) with protease inhibitors), homogenized, and centrifuged for 30 min at 100, 000 g. The lysate supernatant was incubated with normal IgG (control), anti-Daple or dynein IC antibody, and was precipitated by protein G-Sepharose (GE Healthcare), and subsequently solubilized in SDS sample loading buffer. Samples were separated by SDS-PAGE and transferred to PVDF membranes (Millipore). The membranes were blocked with 4% skimmed milk and probed with primary

antibodies. Detection was carried out using HRP-conjugated secondary antibodies (Dako) and visualized using an enhanced chemiluminescence system (Amersham Biosciences).

LV explants culture

LV wall explants were cultured as previously described (Mahuzier et al., 2018) on semipermeable polyester filter inserts (Transwell, 0.4 µm pore size, Corning) in DMEM-Glutamax (Invitrogen) with 10% FBS, 1% penicillin/streptomycin, and 10µM nocodazole (Merck) for 24 h or 20 µM Dynarrestin (R&D Systems) for 12 h (Fig.4C) or 24 h (Fig. 4A). The LV wall of the opposite side of each brain was cultured in DMEM-Glutamax (Invitrogen) with 10% FBS, 1% penicillin/streptomycin, and DMSO as a control.

Antibodies

Protein	Host species	Source	Product number	Dilution
Beta-catenin	Mouse	BD Transduction Laboratories	610153	1:500 (IF)
Beta-catenin	Rabbit	Santa Cruz Biotechnology	Sc-7199	1:100 (IF)
c-Myc	Mouse	Santa Cruz Biotechnology	sc-40	1:500 (IF)
CAMSAP2	Rabbit	Proteintech	17880-1-AP	1:100 (IF)
Daple	Rabbit	IBL	28147	1:100 (IF), 1:1000 (WB)
Dvl1	Mouse	Santa Cruz Biotechnology	sc-8025, sc-8026	1:100 (IF), 1:1000 (WB)
Dynein HC	Mouse	Santa Cruz Biotechnology	Sc-514579	1:1000 (WB)
Dynein IC	Mouse	Millipore	MAB1618	1:100 (IF)
EB3	Rabbit	Cell Signaling Technology	3195	1:500 (IF)

FGFR1OP (FOP)	Mouse	Abnova	H00011116-M01	1:100 (IF)
Fzd6	Goat	R&D Systems	AF1526	1:50 (IF)
Gamma-tubulin	Goat	Santa Cruz Biotechnology	sc-7396	1:500 (IF)
Tyrosinated alpha-tubulin	Rat	abcam	ab6160	1:500 (IF)
Vangl2	Rabbit	Sigma	HPA027043	1:100 (IF)

Statistical analyses

Student's t-test or Mann-Whitney U test (GraphPad Prism 6, GraphPad) was used to compare the means of two experimental groups. Differences were considered statistically significant at $P < 0.05$. To determine the rotational BB orientation for a single ependymal cell, a vector was drawn from the center of FOP dot to the center of the closest γ-tubulin dot in images aligned with the anterior side oriented towards the left, and more than 15 vectors were averaged. Vector angles were measured using Fiji software (Schindelin et al., 2012) and plotted on a circular diagram using the statistical software R (R Core Team, 2019). The resulting sample mean lengths (R/n) and circular variance ($V = 1 - \bar{R}$) for single cells were calculated using the "circular" package (Lund and Agostinelli, 2011) within the R statistical computing environment. Distribution of vector angles for DMSO (control) and Dynarrestin treatments were compared using Watson's two-sample U2 test (R). The means of V for DMSO (control) and Dynarrestin treatments were compared using the Mann-Whitney U test (GraphPad Prism 6).

SUPPLEMENTAL REFERENCES

Lund, U. and Agostinelli, C. (2011). "circular: circular statistics", ht 1 tp://CRAN.R2 project.org/package=circular [assessed 2011.03.26].

Mahuzier, A., Shihavuddin, A., Fournier, C., Lansade, P., Faucourt, M., Menezes, N., Meunier, A., Garfa-Traoré, M., Carlier, M.F., Voituriez, R., et al. (2018). Ependymal cilia beating induces an actin network to protect centrioles against shear stress. Nat Commun *9*, 2279.

R Core Team (2019). R: A language and environment for statistical computing. R Foundation for Statistical Computing, Vienna, Austria. URL https://www.R-project.org/.
Schindelin J, Arganda-Carreras I, Frise E, Kaynig V, Longair M, Pietzsch T, Preibisch S, Rueden C, Saalfeld S, Schmid B, *et al*. (2012). Fiji: an open-source platform for biological-image analysis. Nat Methods. *9*, 676-682.
Skarnes, W.C., Rosen, B., West, A.P., Koutsourakis, M., Bushell, W., Iyer, V., Mujica, A.O., Thomas, M., Harrow, J., Cox, T., et al. (2011). A conditional knockout resource for the genome-wide study of mouse gene function. Nature. 474, 337-342.